



## Measurement of Time-Dependent $CP$ -Violating Asymmetries in $B^0 \rightarrow K_S^0 K_S^0 K_S^0$ Decay

K. Sumisawa,<sup>29,7</sup> Y. Ushiroda,<sup>7</sup> M. Hazumi,<sup>7</sup> K. Abe,<sup>7</sup> K. Abe,<sup>40</sup> I. Adachi,<sup>7</sup> H. Aihara,<sup>42</sup>  
Y. Asano,<sup>46</sup> V. Aulchenko,<sup>1</sup> T. Aushev,<sup>11</sup> A. M. Bakich,<sup>37</sup> U. Bitenc,<sup>12</sup> I. Bizjak,<sup>12</sup>  
S. Blyth,<sup>24</sup> A. Bondar,<sup>1</sup> A. Bozek,<sup>25</sup> M. Bračko,<sup>7,18,12</sup> J. Brodzicka,<sup>25</sup> T. E. Browder,<sup>6</sup>  
Y. Chao,<sup>24</sup> A. Chen,<sup>22</sup> K.-F. Chen,<sup>24</sup> W. T. Chen,<sup>22</sup> B. G. Cheon,<sup>3</sup> R. Chistov,<sup>11</sup> Y. Choi,<sup>36</sup>  
A. Chuvikov,<sup>32</sup> S. Cole,<sup>37</sup> J. Dalseno,<sup>19</sup> M. Danilov,<sup>11</sup> M. Dash,<sup>47</sup> A. Drutskoy,<sup>4</sup>  
S. Eidelman,<sup>1</sup> Y. Enari,<sup>20</sup> F. Fang,<sup>6</sup> S. Fratina,<sup>12</sup> N. Gabyshev,<sup>1</sup> A. Garmash,<sup>32</sup>  
T. Gershon,<sup>7</sup> G. Gokhroo,<sup>38</sup> B. Golob,<sup>17,12</sup> A. Gorišek,<sup>12</sup> J. Haba,<sup>7</sup> K. Hara,<sup>7</sup> T. Hara,<sup>29</sup>  
H. Hayashii,<sup>21</sup> T. Higuchi,<sup>7</sup> T. Hokuue,<sup>20</sup> Y. Hoshi,<sup>40</sup> S. Hou,<sup>22</sup> W.-S. Hou,<sup>24</sup> Y. B. Hsiung,<sup>24</sup>  
T. Iijima,<sup>20</sup> A. Imoto,<sup>21</sup> K. Inami,<sup>20</sup> A. Ishikawa,<sup>7</sup> H. Ishino,<sup>43</sup> R. Itoh,<sup>7</sup> M. Iwasaki,<sup>42</sup>  
Y. Iwasaki,<sup>7</sup> J. H. Kang,<sup>48</sup> J. S. Kang,<sup>14</sup> S. U. Kataoka,<sup>21</sup> N. Katayama,<sup>7</sup> H. Kawai,<sup>2</sup>  
T. Kawasaki,<sup>27</sup> H. R. Khan,<sup>43</sup> H. Kichimi,<sup>7</sup> H. J. Kim,<sup>15</sup> H. O. Kim,<sup>36</sup> S. K. Kim,<sup>35</sup>  
S. M. Kim,<sup>36</sup> K. Kinoshita,<sup>4</sup> S. Korpar,<sup>18,12</sup> P. Križan,<sup>17,12</sup> P. Krokovny,<sup>1</sup> R. Kulasiri,<sup>4</sup>  
S. Kumar,<sup>30</sup> C. C. Kuo,<sup>22</sup> A. Kusaka,<sup>42</sup> A. Kuzmin,<sup>1</sup> Y.-J. Kwon,<sup>48</sup> J. S. Lange,<sup>5</sup>  
G. Leder,<sup>10</sup> T. Lesiak,<sup>25</sup> S.-W. Lin,<sup>24</sup> F. Mandl,<sup>10</sup> D. Marlow,<sup>32</sup> T. Matsumoto,<sup>44</sup>  
A. Matyja,<sup>25</sup> W. Mitaroff,<sup>10</sup> K. Miyabayashi,<sup>21</sup> H. Miyake,<sup>29</sup> H. Miyata,<sup>27</sup> R. Mizuk,<sup>11</sup>  
T. Nagamine,<sup>41</sup> Y. Nagasaka,<sup>8</sup> E. Nakano,<sup>28</sup> M. Nakao,<sup>7</sup> Z. Natkaniec,<sup>25</sup> S. Nishida,<sup>7</sup>  
O. Nitoh,<sup>45</sup> T. Nozaki,<sup>7</sup> S. Ogawa,<sup>39</sup> T. Ohshima,<sup>20</sup> T. Okabe,<sup>20</sup> S. Okuno,<sup>13</sup> S. L. Olsen,<sup>6</sup>  
Y. Onuki,<sup>27</sup> W. Ostrowicz,<sup>25</sup> H. Ozaki,<sup>7</sup> C. W. Park,<sup>36</sup> H. Park,<sup>15</sup> N. Parslow,<sup>37</sup>  
L. S. Peak,<sup>37</sup> R. Pestotnik,<sup>12</sup> L. E. Pilonen,<sup>47</sup> M. Rozanska,<sup>25</sup> H. Sagawa,<sup>7</sup> Y. Sakai,<sup>7</sup>  
T. R. Sarangi,<sup>7</sup> N. Sato,<sup>20</sup> T. Schietinger,<sup>16</sup> O. Schneider,<sup>16</sup> R. Seuster,<sup>6</sup> M. E. Sevier,<sup>19</sup>  
H. Shibuya,<sup>39</sup> V. Sidorov,<sup>1</sup> J. B. Singh,<sup>30</sup> A. Somov,<sup>4</sup> R. Stamen,<sup>7</sup> S. Stanič,<sup>46,\*</sup>  
M. Starič,<sup>12</sup> T. Sumiyoshi,<sup>44</sup> S. Suzuki,<sup>33</sup> O. Tajima,<sup>7</sup> F. Takasaki,<sup>7</sup> K. Tamai,<sup>7</sup>  
N. Tamura,<sup>27</sup> M. Tanaka,<sup>7</sup> Y. Teramoto,<sup>28</sup> X. C. Tian,<sup>31</sup> K. Trabelsi,<sup>6</sup> T. Tsuboyama,<sup>7</sup>  
T. Tsukamoto,<sup>7</sup> S. Uehara,<sup>7</sup> T. Uglov,<sup>11</sup> K. Ueno,<sup>24</sup> S. Uno,<sup>7</sup> P. Urquijo,<sup>19</sup> G. Varner,<sup>6</sup>  
K. E. Varvell,<sup>37</sup> S. Villa,<sup>16</sup> C. C. Wang,<sup>24</sup> C. H. Wang,<sup>23</sup> M.-Z. Wang,<sup>24</sup> Q. L. Xie,<sup>9</sup>  
B. D. Yabsley,<sup>47</sup> A. Yamaguchi,<sup>41</sup> H. Yamamoto,<sup>41</sup> Y. Yamashita,<sup>26</sup> M. Yamauchi,<sup>7</sup>  
Heyoung Yang,<sup>35</sup> J. Zhang,<sup>7</sup> L. M. Zhang,<sup>34</sup> Z. P. Zhang,<sup>34</sup> V. Zhilich,<sup>1</sup> and D. Žontar<sup>17,12</sup>

(The Belle Collaboration)

<sup>1</sup>*Budker Institute of Nuclear Physics, Novosibirsk*

<sup>2</sup>*Chiba University, Chiba*

<sup>3</sup>*Chonnam National University, Kwangju*

<sup>4</sup>*University of Cincinnati, Cincinnati, Ohio 45221*

<sup>5</sup>*University of Frankfurt, Frankfurt*

<sup>6</sup>*University of Hawaii, Honolulu, Hawaii 96822*

- <sup>7</sup>High Energy Accelerator Research Organization (KEK), Tsukuba  
<sup>8</sup>Hiroshima Institute of Technology, Hiroshima  
<sup>9</sup>Institute of High Energy Physics, Chinese Academy of Sciences, Beijing  
<sup>10</sup>Institute of High Energy Physics, Vienna  
<sup>11</sup>Institute for Theoretical and Experimental Physics, Moscow  
<sup>12</sup>J. Stefan Institute, Ljubljana  
<sup>13</sup>Kanagawa University, Yokohama  
<sup>14</sup>Korea University, Seoul  
<sup>15</sup>Kyungpook National University, Taegu  
<sup>16</sup>Swiss Federal Institute of Technology of Lausanne, EPFL, Lausanne  
<sup>17</sup>University of Ljubljana, Ljubljana  
<sup>18</sup>University of Maribor, Maribor  
<sup>19</sup>University of Melbourne, Victoria  
<sup>20</sup>Nagoya University, Nagoya  
<sup>21</sup>Nara Women's University, Nara  
<sup>22</sup>National Central University, Chung-li  
<sup>23</sup>National United University, Miao Li  
<sup>24</sup>Department of Physics, National Taiwan University, Taipei  
<sup>25</sup>H. Niewodniczanski Institute of Nuclear Physics, Krakow  
<sup>26</sup>Nihon Dental College, Niigata  
<sup>27</sup>Niigata University, Niigata  
<sup>28</sup>Osaka City University, Osaka  
<sup>29</sup>Osaka University, Osaka  
<sup>30</sup>Panjab University, Chandigarh  
<sup>31</sup>Peking University, Beijing  
<sup>32</sup>Princeton University, Princeton, New Jersey 08544  
<sup>33</sup>Saga University, Saga  
<sup>34</sup>University of Science and Technology of China, Hefei  
<sup>35</sup>Seoul National University, Seoul  
<sup>36</sup>Sungkyunkwan University, Suwon  
<sup>37</sup>University of Sydney, Sydney NSW  
<sup>38</sup>Tata Institute of Fundamental Research, Bombay  
<sup>39</sup>Toho University, Funabashi  
<sup>40</sup>Tohoku Gakuin University, Tagajo  
<sup>41</sup>Tohoku University, Sendai  
<sup>42</sup>Department of Physics, University of Tokyo, Tokyo  
<sup>43</sup>Tokyo Institute of Technology, Tokyo  
<sup>44</sup>Tokyo Metropolitan University, Tokyo  
<sup>45</sup>Tokyo University of Agriculture and Technology, Tokyo  
<sup>46</sup>University of Tsukuba, Tsukuba  
<sup>47</sup>Virginia Polytechnic Institute and State University, Blacksburg, Virginia 24061  
<sup>48</sup>Yonsei University, Seoul

(Dated: August 22, 2019)

## Abstract

We present a measurement of  $CP$ -violation parameters in the  $B^0 \rightarrow K_S^0 K_S^0 K_S^0$  decay based on a sample of  $275 \times 10^6$   $B\bar{B}$  pairs collected at the  $\Upsilon(4S)$  resonance with the Belle detector at the KEKB energy-asymmetric  $e^+e^-$  collider. One neutral  $B$  meson is fully reconstructed in the decay  $B^0 \rightarrow K_S^0 K_S^0 K_S^0$ , and the flavor of the accompanying  $B$  meson is identified from its decay products.  $CP$ -violation parameters are obtained from the asymmetry in the distributions of the proper-time interval between the two  $B$  decays:  $\mathcal{S} = +1.26 \pm 0.68(\text{stat}) \pm 0.20(\text{syst})$  and  $\mathcal{A} = +0.54 \pm 0.34(\text{stat}) \pm 0.09(\text{syst})$ .

PACS numbers: 11.30.Er, 12.15.Hh, 13.25.Hw

---

\*on leave from Nova Gorica Polytechnic, Nova Gorica

In the Standard Model (SM),  $CP$  violation arises from the Kobayashi-Maskawa phase [1] in the weak-interaction quark-mixing matrix. In particular, the SM predicts to a good approximation that  $\mathcal{S} = -\xi_f \sin 2\phi_1$  and  $\mathcal{A} = 0$  for both  $b \rightarrow c\bar{c}s$  and  $b \rightarrow s\bar{q}q$  transitions, where  $\mathcal{S}$  ( $\mathcal{A}$ ) is a parameter for mixing-induced (direct)  $CP$  violation [2],  $\xi_f = +1(-1)$  corresponds to  $CP$ -even (-odd) final states, and  $\phi_1$  is one of angles of the Unitarity Triangle. Measurements of time-dependent  $CP$  asymmetries in  $B^0 \rightarrow J/\psi K_S^0$  [3] and related decay modes, which are governed by the  $b \rightarrow c\bar{c}s$  transition, by the Belle [4, 5] and BaBar [6] collaborations already determine  $\sin 2\phi_1$  rather precisely; the present world average value is  $\sin 2\phi_1 = +0.726 \pm 0.037$  [7].

$CP$ -violation parameters in the flavor-changing  $b \rightarrow s$  transition are sensitive to phenomena at a very high-energy scale [8, 9]. Belle measurements [10] in the decay modes  $B^0 \rightarrow \phi K_S^0$ ,  $\phi K_L^0$ ,  $K^+ K^- K_S^0$ ,  $f_0(980) K_S^0$ ,  $\eta' K_S^0$ ,  $\omega K_S^0$ , and  $K_S^0 \pi^0$ , which are dominated by the  $b \rightarrow s\bar{q}q$  transition, yield  $\sin 2\phi_1 = +0.43_{-0.11}^{+0.12}$  when all the modes are combined. Measurements by the BaBar collaboration also yield a similar deviation [7, 11]. To elucidate the difference in  $CP$  asymmetries between  $b \rightarrow s\bar{q}q$  and  $b \rightarrow c\bar{c}s$  transitions, it is essential to examine additional modes that may be sensitive to the same  $b \rightarrow s$  amplitude.

The  $B^0$  decay to  $K_S^0 K_S^0 K_S^0$ , which is a  $\xi_f = +1$  state, is one of the most promising modes for this purpose [12]. Since there is no  $u$  quark in the final state, the decay is dominated by the  $b \rightarrow s\bar{s}s$  transition. Its branching fraction  $\mathcal{B}(B^0 \rightarrow K_S^0 K_S^0 K_S^0) = (4.2_{-1.3}^{+1.6} \pm 0.8) \times 10^{-6}$  was reported by Belle [13]. In this Letter, we describe a measurement of  $CP$  asymmetries in the  $B^0 \rightarrow K_S^0 K_S^0 K_S^0$  decay.

In the decay chain  $\Upsilon(4S) \rightarrow B^0 \bar{B}^0 \rightarrow f_{CP} f_{\text{tag}}$ , where one of the  $B$  mesons decays at time  $t_{CP}$  to a  $CP$  eigenstate  $f_{CP}$  and the other decays at time  $t_{\text{tag}}$  to a final state  $f_{\text{tag}}$  that distinguishes between  $B^0$  and  $\bar{B}^0$ , the decay rate has a time dependence given by

$$\mathcal{P}(\Delta t) = \frac{e^{-|\Delta t|/\tau_{B^0}}}{4\tau_{B^0}} \left\{ 1 + q \cdot \left[ \mathcal{S} \sin(\Delta m_d \Delta t) + \mathcal{A} \cos(\Delta m_d \Delta t) \right] \right\}. \quad (1)$$

Here  $\tau_{B^0}$  is the  $B^0$  lifetime,  $\Delta m_d$  is the mass difference between the two  $B^0$  mass eigenstates,  $\Delta t$  is the time difference  $t_{CP} - t_{\text{tag}}$ , and the  $b$ -flavor charge is  $q = +1$  ( $-1$ ) when the tagging  $B$  meson is a  $B^0$  ( $\bar{B}^0$ ).

At the KEKB energy-asymmetric  $e^+e^-$  (3.5 on 8.0 GeV) collider [14], the  $\Upsilon(4S)$  resonance is produced with a Lorentz boost of  $\beta\gamma = 0.425$  along the  $z$  direction which is antiparallel to the positron beamline. Since the  $B^0$  and  $\bar{B}^0$  mesons are approximately at rest in the  $\Upsilon(4S)$  center-of-mass system (cms),  $\Delta t$  can be determined from the displacement in  $z$  between the  $f_{CP}$  and  $f_{\text{tag}}$  decay vertices:  $\Delta t \simeq (z_{CP} - z_{\text{tag}})/(\beta\gamma c) \equiv \Delta z/(\beta\gamma c)$ .

The Belle detector [15] is a large-solid-angle magnetic spectrometer that consists of a silicon vertex detector (SVD), a 50-layer central drift chamber, an array of aerogel threshold Cherenkov counters, a barrel-like arrangement of time-of-flight scintillation counters, an electromagnetic calorimeter (ECL) and an iron flux-return instrumented to detect  $K_L^0$  mesons and to identify muons. A 2.0 cm radius beampipe and a 3-layer SVD (SVD-I) were used for a  $140 \text{ fb}^{-1}$  data sample, while a 1.5 cm radius beampipe, a 4-layer silicon detector (SVD-II) [16] and a small-cell inner drift chamber were used for an additional  $113 \text{ fb}^{-1}$  data sample. In total  $275 \times 10^6$   $B\bar{B}$  pairs were accumulated.

We reconstruct the  $B^0 \rightarrow K_S^0 K_S^0 K_S^0$  decay in the  $K_S^{+-} K_S^{+-} K_S^{+-}$  or  $K_S^{+-} K_S^{+-} K_S^{00}$  final state, where the  $\pi^+ \pi^-$  ( $\pi^0 \pi^0$ ) state from a  $K_S^0$  decay is denoted as  $K_S^{+-}$  ( $K_S^{00}$ ). Pairs of

oppositely charged tracks with the  $\pi^+\pi^-$  invariant mass within  $0.012 \text{ GeV}/c^2$  ( $\simeq 3\sigma$ ) of the nominal  $K_S^0$  mass are used to reconstruct  $K_S^{+-}$  candidates. The  $\pi^+\pi^-$  vertex is required to be displaced from the interaction point (IP) by a minimum transverse distance of 0.22 cm for candidates with  $p > 1.5 \text{ GeV}/c$  and 0.08 cm for those with  $p < 1.5 \text{ GeV}/c$ , where  $p$  is the momentum of  $K_S^0$ . The angle in the transverse plane between the  $K_S^0$  momentum vector and the direction defined by the  $K_S^0$  vertex and the IP should be less than 0.03 rad (0.1 rad) for the high (low) momentum candidates. The mismatch in the  $z$  direction at the  $K_S^0$  vertex point for the two charged pion tracks should be less than 2.4 cm (1.8 cm) for the high (low) momentum candidates. After two good  $K_S^{+-}$  candidates have been found which satisfy the criteria given above, looser requirements are applied for the third  $K_S^{+-}$  candidate. The requirement on the transverse direction matching is relaxed to 0.2 rad (0.4 rad for low momentum candidates), and the mismatch of the two charged pions in the  $z$  direction is required to be less than 5 cm (1 cm if both pions have hits in the SVD).

To select  $K_S^{00}$  candidates, we reconstruct  $\pi^0$  candidates from pairs of photons with  $E_\gamma > 0.05 \text{ GeV}$ , where  $E_\gamma$  is the photon energy measured with the ECL. The reconstructed  $\pi^0$  candidate is required to have an invariant mass between 0.08 and  $0.15 \text{ GeV}/c^2$  and momentum above  $0.1 \text{ GeV}/c$ .  $K_S^{00}$  candidates are required to have an invariant mass between 0.47 and  $0.52 \text{ GeV}/c^2$ , and a fit is performed with constraints on the  $K_S^0$  vertex and  $\pi^0$  masses to improve the  $\pi^0\pi^0$  invariant mass resolution. The  $K_S^{00}$  candidate is combined with two good  $K_S^{+-}$  candidates to reconstruct a  $B^0$  meson.

To identify  $B^0 \rightarrow K_S^0 K_S^0 K_S^0$  decays, we use the energy difference  $\Delta E \equiv E_B^{\text{cms}} - E_{\text{beam}}^{\text{cms}}$  and the beam-energy constrained mass  $M_{\text{bc}} \equiv \sqrt{(E_{\text{beam}}^{\text{cms}})^2 - (p_B^{\text{cms}})^2}$ , where  $E_{\text{beam}}^{\text{cms}}$  is the beam energy in the cms, and  $E_B^{\text{cms}}$  and  $p_B^{\text{cms}}$  are the cms energy and momentum of the reconstructed  $B$  candidate, respectively. The  $B^0$  meson signal region is defined as  $|\Delta E| < 0.10 \text{ GeV}$  for  $B^0 \rightarrow K_S^{+-} K_S^{+-} K_S^{+-}$ ,  $-0.15 < \Delta E < 0.10 \text{ GeV}$  for  $B^0 \rightarrow K_S^{+-} K_S^{+-} K_S^{00}$ , and  $5.27 < M_{\text{bc}} < 5.29 \text{ GeV}/c^2$  for both decays. To suppress the  $e^+e^- \rightarrow q\bar{q}$  continuum background ( $q = u, d, s, c$ ), we form a signal over background likelihood ratio  $\mathcal{R}_{\text{s/b}}$  by combining likelihoods for two quantities; a Fisher discriminant of modified Fox-Wolfram moments [17], and the cosine of the cms  $B^0$  flight direction. The requirement for  $\mathcal{R}_{\text{s/b}}$  depends both on the decay mode and on the flavor-tagging quality; after applying all other cuts, this rejects 94% of the  $q\bar{q}$  background while retaining 75% of the signal.

If both  $B^0 \rightarrow K_S^{+-} K_S^{+-} K_S^{+-}$  and  $K_S^{+-} K_S^{+-} K_S^{00}$  candidates are found in the same event, we choose the  $B^0 \rightarrow K_S^{+-} K_S^{+-} K_S^{+-}$  candidate. When multiple  $B^0 \rightarrow K_S^{+-} K_S^{+-} K_S^{+-}$  candidates are found, we prioritize those with three good  $K_S^{+-}$  candidates. If more than one candidate still remain, we select the one with the smallest value for  $\sum(\Delta M_{K_S^{+-}})^2$ , where  $\Delta M_{K_S^{+-}}$  is the difference between the reconstructed and nominal mass of  $K_S^{+-}$ . For multiple  $B^0 \rightarrow K_S^{+-} K_S^{+-} K_S^{00}$  candidates, we select the  $K_S^{+-} K_S^{+-}$  pair that has the smallest  $\sum(\Delta M_{K_S^{+-}})^2$  value and the  $K_S^{00}$  candidate with the minimum  $\chi^2$  of the constrained fit.

We reject  $K_S^0 K_S^0 K_S^0$  candidates if they are consistent with  $B^0 \rightarrow \chi_{c0} K_S^0 \rightarrow (K_S^0 K_S^0) K_S^0$  or  $B^0 \rightarrow D^0 K_S^0 \rightarrow (K_S^0 K_S^0) K_S^0$  decays, i.e. if one of the  $K_S^0$  pairs has an invariant mass within  $\pm 2\sigma$  of the  $\chi_{c0}$  mass or  $D^0$  mass, where  $\sigma$  is the  $K_S^0 K_S^0$  mass resolution.

Figure 1 shows the  $M_{\text{bc}}$  and  $\Delta E$  distributions for the reconstructed  $B^0 \rightarrow K_S^0 K_S^0 K_S^0$  candidates after flavor tagging. The signal yield is determined from an unbinned two-dimensional maximum-likelihood fit to the  $\Delta E$ - $M_{\text{bc}}$  distribution. The  $K_S^{+-} K_S^{+-} K_S^{+-}$  signal distribution is modeled with a Gaussian function (a sum of two Gaussian functions) for  $M_{\text{bc}}$  ( $\Delta E$ ). For  $B^0 \rightarrow K_S^{+-} K_S^{+-} K_S^{00}$  decay, the signal is modeled with a two-dimensional smoothed histogram obtained from Monte Carlo (MC) events. For the continuum background, we use

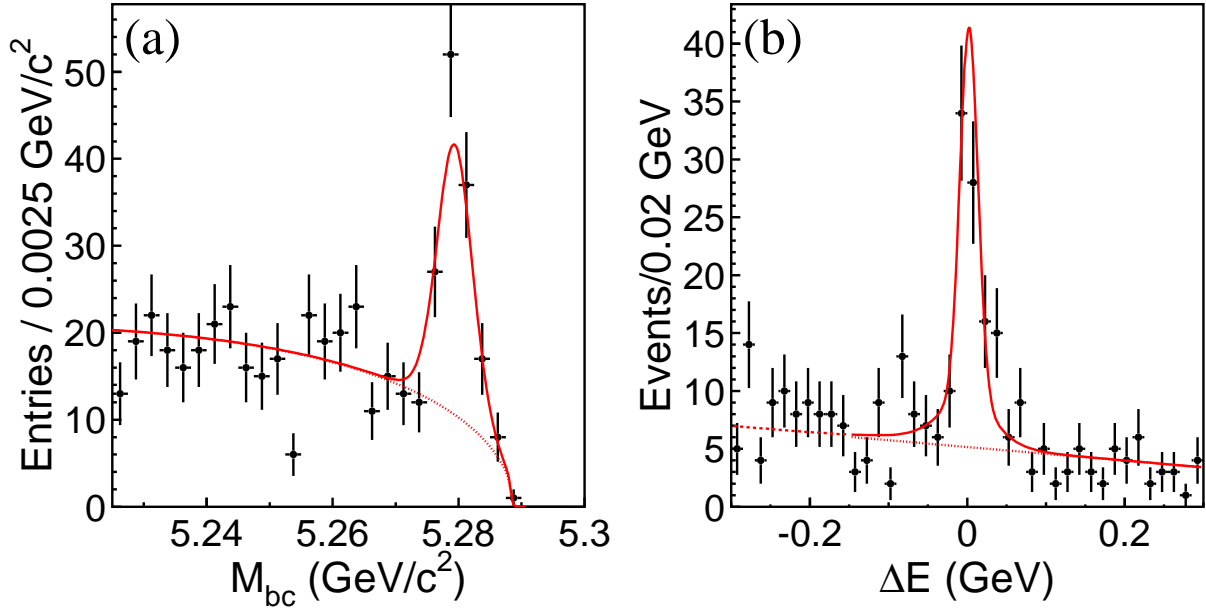


FIG. 1: (a)  $M_{bc}$  distribution within the  $\Delta E$  signal region, (b)  $\Delta E$  distribution within the  $M_{bc}$  signal region. Solid curves show the fit to signal plus background distributions, and dashed curves show the background contributions.

the ARGUS parameterization [18] for  $M_{bc}$  and a linear function for  $\Delta E$ . The fits after flavor tagging yield  $72 \pm 10$   $B^0 \rightarrow K_S^{+-} K_S^{+-} K_S^{+-}$  events and  $16 \pm 8$   $B^0 \rightarrow K_S^{+-} K_S^{+-} K_S^{00}$  events for a total of  $88 \pm 13$   $B^0 \rightarrow K_S^0 K_S^0 K_S^0$  events in the signal region, where the errors are statistical only. The obtained purity is 0.56 for the  $K_S^{+-} K_S^{+-} K_S^{+-}$  and 0.40 for the  $K_S^{+-} K_S^{+-} K_S^{00}$  channels. We use events outside the signal region as well as a large MC sample to study the background components. The dominant background is from continuum. The contamination of  $B^0 \rightarrow \chi_{c0} K_S^0$  events in the  $B^0 \rightarrow K_S^0 K_S^0 K_S^0$  sample is small (less than 2.6% at 90% C.L.). The contributions from other  $B\bar{B}$  events are negligibly small. The influence of these backgrounds is treated as a source of systematic uncertainty in the  $CP$  asymmetry measurement. Backgrounds from the decay  $B^0 \rightarrow D^0 K_S^0$  are found to be negligible.

The  $b$ -flavor of the accompanying  $B$  meson is identified from inclusive properties of particles that are not associated with the reconstructed  $B^0 \rightarrow K_S^0 K_S^0 K_S^0$  candidates. The algorithm for flavor tagging is described in detail elsewhere [19]. We use two parameters,  $q$  defined in Eq. (1) and  $r$ , to represent the tagging information. The parameter  $r$  is an event-by-event, MC-determined flavor-tagging dilution factor that ranges from  $r = 0$  for no flavor discrimination to  $r = 1$  for unambiguous flavor assignment. It is used only to sort data into six  $r$  intervals. The wrong tag fractions  $w$  for each of the  $r$  intervals and their differences  $\Delta w$  for  $B^0$  and  $\bar{B}^0$  decays are determined from data [10].

The vertex position for  $B^0 \rightarrow K_S^0 K_S^0 K_S^0$  decays is obtained using  $K_S^{+-}$  trajectories and a constraint on the IP; the IP profile ( $\sigma_x \simeq 100 \mu\text{m}$ ,  $\sigma_y \simeq 5 \mu\text{m}$ ,  $\sigma_z \simeq 3 \text{mm}$ ) is convolved with finite  $B^0$  flight length in the plane perpendicular to the  $z$  axis. To reconstruct the  $K_S^{+-}$  trajectory with sufficient resolution, both charged pions from the  $K_S^0$  decay are required to have enough SVD hits; at least one layer with hits on both sides and at least one additional  $z$  hit in other layers for SVD-I, and at least two layers with hits on both sides for SVD-II. The reconstruction efficiency depends both on the  $K_S^{+-}$  momentum and on the SVD geometry.

The vertex efficiencies with SVD-II (86% for  $K_S^{+-} K_S^{+-} K_S^{+-}$  and 74% for  $K_S^{+-} K_S^{+-} K_S^{00}$ ) are higher than those with SVD-I (79% for  $K_S^{+-} K_S^{+-} K_S^{+-}$  and 62% for  $K_S^{+-} K_S^{+-} K_S^{00}$ ) because of the larger outer radius and the additional detector layer. The typical vertex resolution is about  $97 \mu\text{m}$  ( $113 \mu\text{m}$ ) for SVD-I (SVD-II) when two or three  $K_S^{+-}$  candidates can be used. The resolution is worse when only one  $K_S^{+-}$  can be used; the typical value is  $152 \mu\text{m}$  ( $168 \mu\text{m}$ ) for SVD-I (SVD-II), which is comparable to the  $f_{\text{tag}}$  vertex resolution. The determination of the vertex of the  $f_{\text{tag}}$  final state is the same as the  $B^0 \rightarrow \phi K_S^0$  analysis, and is described in detail elsewhere [10, 20].

We determine  $\mathcal{S}$  and  $\mathcal{A}$  by performing an unbinned maximum-likelihood fit to the observed  $\Delta t$  distribution. The probability density function (PDF) expected for the signal distribution,  $\mathcal{P}_{\text{sig}}(\Delta t; \mathcal{S}, \mathcal{A}, q, w, \Delta w)$ , is given by Eq. (1) after incorporating the effect of incorrect flavor assignment. The distribution is convolved with the proper-time interval resolution function,  $R_{\text{sig}}$ , which is a function of event-by-event vertex errors.

We find from MC simulation that universal  $R_{\text{sig}}$  parameters used for measurements of  $CP$  asymmetries in the  $B^0 \rightarrow J/\psi K_S^0$  and related decays [5, 20] approximately describe the resolution for the  $B^0 \rightarrow K_S^0 K_S^0 K_S^0$  decay. To account for differences between  $K_S^{+-}$  trajectories and charged tracks, additional parameters that rescale vertex errors are introduced. When only one  $K_S^{+-}$  is used in the vertex fit, these parameters are determined from a fit to the  $\Delta t$  distribution of  $B^0 \rightarrow J/\psi K_S^0$  candidates, where only the  $K_S^0$  and the IP constraint are used for the vertex reconstruction. The procedure is the same as that for the  $B^0 \rightarrow K_S^0 \pi^0$  decay and is described elsewhere [10]. For events with two or three  $K_S^{+-}$  used in the vertexing, we also find from MC simulation that the resolution is well described by the same  $R_{\text{sig}}$  parameterization with an additional correction function that depends on the number of  $K_S^{+-}$  decays used for the vertex reconstruction. The form of this correction function is determined from a study using MC simulation.

We determine the following likelihood value for each event  $i$ :

$$\begin{aligned}
P_i = & (1 - f_{\text{ol}}) \int \left[ f_{\text{sig}} \mathcal{P}_{\text{sig}}(\Delta t') R_{\text{sig}}(\Delta t_i - \Delta t') \right. \\
& + (1 - f_{\text{sig}}) \mathcal{P}_{\text{bkg}}(\Delta t') R_{\text{bkg}}(\Delta t_i - \Delta t') \left. \right] d(\Delta t') \\
& + f_{\text{ol}} P_{\text{ol}}(\Delta t_i),
\end{aligned} \tag{2}$$

where  $P_{\text{ol}}$  is a broad Gaussian function that represents an outlier component with a small fraction  $f_{\text{ol}}$  [20]. The signal probability  $f_{\text{sig}}$  is calculated on an event-by-event basis from the function obtained by the  $\Delta E$ - $M_{\text{bc}}$  two-dimensional fit used to extract the signal yield. A PDF for background events,  $\mathcal{P}_{\text{bkg}}$ , is modeled as a sum of exponential and prompt components, and is convolved with a sum of two Gaussians  $R_{\text{bkg}}$ . All parameters in  $\mathcal{P}_{\text{bkg}}$  and  $R_{\text{bkg}}$  are determined by the fit to the  $\Delta t$  distribution of a background-enhanced control sample, i.e. events outside of the  $\Delta E$ - $M_{\text{bc}}$  signal region. We fix  $\tau_{B^0}$  and  $\Delta m_d$  at their world-average values [21]. In order to reduce the statistical error on  $\mathcal{A}$ , we include events without vertex information. The likelihood value in this case is obtained from the function of Eq. (2) integrated over  $\Delta t_i$ .

The only free parameters in the final fit are  $\mathcal{S}$  and  $\mathcal{A}$ , which are determined by maximizing the likelihood function  $L = \prod_i P_i(\Delta t_i; \mathcal{S}, \mathcal{A})$  where the product is over all events. An unbinned maximum likelihood fit to the  $167 B^0 \rightarrow K_S^0 K_S^0 K_S^0$  candidates, containing  $88 \pm 13 K_S^0 K_S^0 K_S^0$  signal events, yields

$$\mathcal{S} = +1.26 \pm 0.68(\text{stat}) \pm 0.20(\text{syst}),$$

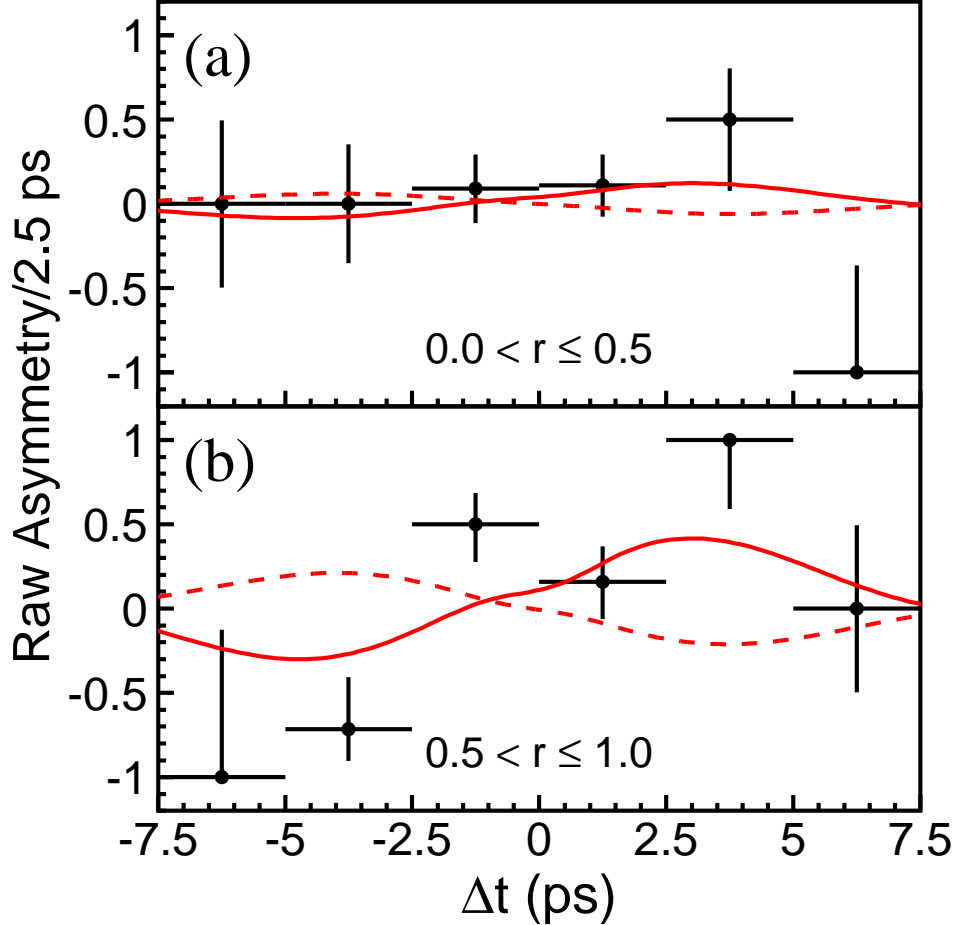


FIG. 2: Raw asymmetry in each  $\Delta t$  bin with (a)  $0 < r \leq 0.5$  and (b)  $0.5 < r \leq 1.0$ . The solid curves show the result of the unbinned maximum-likelihood fit. The dashed curves show the SM expectation with  $(\mathcal{S}, \mathcal{A}) = (-0.73, 0)$ . The numbers of candidate events used for the  $\mathcal{S}$  measurement are 65 for (a)  $0 < r \leq 0.5$  and 52 for (b)  $0.5 < r \leq 1.0$ .

$$\mathcal{A} = +0.54 \pm 0.34(\text{stat}) \pm 0.09(\text{syst}).$$

We define the raw asymmetry in each  $\Delta t$  interval by  $(N_+ - N_-)/(N_+ + N_-)$ , where  $N_{+(-)}$  is the number of observed candidates with  $q = +1(-1)$ . The raw asymmetries in two regions of the flavor-tagging parameter  $r$  are shown in Fig. 2. Note that these are simple projections onto the  $\Delta t$  axis and do not reflect other event-by-event information (such as the signal fraction, the wrong tag fraction and the vertex resolution), which is in fact used in the unbinned maximum-likelihood fit for  $\mathcal{S}$  and  $\mathcal{A}$ .

The systematic error is primarily due to the resolution function ( $\pm 0.12$  for  $\mathcal{S}$  and  $\pm 0.04$  for  $\mathcal{A}$ ), the background fractions ( $\pm 0.10$  for  $\mathcal{S}$  and  $\pm 0.03$  for  $\mathcal{A}$ ), fit bias ( $\pm 0.08$  for  $\mathcal{S}$  and  $\pm 0.05$  for  $\mathcal{A}$ ), and background modeling ( $\pm 0.08$  for  $\mathcal{S}$  and  $\pm 0.01$  for  $\mathcal{A}$ ). Other sources of systematic error are uncertainties in the wrong tag fraction ( $\pm 0.04$  for  $\mathcal{S}$  and  $\pm 0.01$  for  $\mathcal{A}$ ), physics parameters  $\Delta m_d$  and  $\tau_{B^0}$  ( $\pm 0.01$  for  $\mathcal{S}$  and  $\pm 0.01$  for  $\mathcal{A}$ ), the vertexing ( $\pm 0.02$  for



$\mathcal{S}$  and  $\pm 0.05$  for  $\mathcal{A}$ ), and the effect of tag side interference [22] ( $\pm 0.02$  for  $\mathcal{S}$  and  $\pm 0.02$  for  $\mathcal{A}$ ). We add each contribution in quadrature to obtain the total systematic errors.

Various cross-checks of the measurement are performed. We reconstruct  $B^\pm \rightarrow K_S^0 K_S^0 K^\pm$  decays without using the charged kaon for the vertex reconstruction and apply the same fit procedure. We obtain  $\mathcal{S}_{K_S^0 K_S^0 K^\pm} = +0.33_{-0.45}^{+0.39}(\text{stat})$  and  $\mathcal{A}_{K_S^0 K_S^0 K^\pm} = -0.32 \pm 0.28(\text{stat})$ , which are consistent with no  $CP$  asymmetry. MC pseudo-experiments are generated to perform ensemble tests. We find that the statistical errors obtained in our measurement are all consistent with the expectations from the ensemble tests. We apply the same procedure to the  $B^0 \rightarrow J/\psi K_S^0$  sample without  $J/\psi$  daughter tracks for vertex reconstruction. We obtain  $\mathcal{S}_{J/\psi K_S^0} = +0.68 \pm 0.10(\text{stat})$  and  $\mathcal{A}_{J/\psi K_S^0} = +0.02 \pm 0.04(\text{stat})$ , which are in good agreement with the world average values [7]. We conclude that the vertex resolution for the  $B^0 \rightarrow K_S^0 K_S^0 K_S^0$  decay is well understood.

We use a frequentist approach [23] to determine the statistical significance of the deviation from the SM. From 1-dimensional confidence intervals for  $\mathcal{S}$ , the case with  $\mathcal{S} = -0.73$  for  $B^0 \rightarrow K_S^0 K_S^0 K_S^0$  is ruled out at a 99.7% confidence level, equivalent to  $2.9\sigma$  significance for Gaussian errors.

In summary, we have performed the measurement of  $CP$ -violation parameters in the  $B^0 \rightarrow K_S^0 K_S^0 K_S^0$  decay based on a sample of  $275 \times 10^6 B\bar{B}$  pairs. The decay is dominated by the  $b \rightarrow s$  flavor-changing neutral current and the  $K_S^0 K_S^0 K_S^0$  final state is a  $CP$  eigenstate. It is therefore sensitive to a possible new  $CP$ -violating phase beyond the SM. The result differs from the SM expectation by 2.9 standard deviations.

We thank the KEKB group for the excellent operation of the accelerator, the KEK cryogenics group for the efficient operation of the solenoid, and the KEK computer group and the NII for valuable computing and Super-SINET network support. We acknowledge support from MEXT and JSPS (Japan); ARC and DEST (Australia); NSFC (contract No. 10175071, China); DST (India); the BK21 program of MOEHRD and the CHEP SRC program of KOSEF (Korea); KBN (contract No. 2P03B 01324, Poland); MIST (Russia); MHEST (Slovenia); SNSF (Switzerland); NSC and MOE (Taiwan); and DOE (USA).

*Note added.*—As we were preparing to submit this paper, we became aware of a paper from the BaBar collaboration [24] which reports on the branching fraction and  $CP$  asymmetries in the  $B^0 \rightarrow K_S^0 K_S^0 K_S^0$  decay.

- 
- [1] M. Kobayashi and T. Maskawa, Prog. Theor. Phys. **49**, 652 (1973).
  - [2] A. B. Carter and A. I. Sanda, Phys. Rev. D **23**, 1567 (1981); I. I. Bigi and A. I. Sanda, Nucl. Phys. **B193**, 85 (1981).
  - [3] Throughout this paper, the inclusion of the charge conjugate decay mode is implied unless otherwise stated.
  - [4] Belle Collaboration, K. Abe *et al.*, Phys. Rev. Lett. **87**, 091802 (2001); Phys. Rev. D **66**, 032007 (2002); Phys. Rev. D **66**, 071102 (2002).
  - [5] Belle Collaboration, K. Abe *et al.*, Phys. Rev. D **71**, 072003 (2005).
  - [6] BaBar Collaboration, B. Aubert *et al.*, Phys. Rev. Lett. **87**, 091801 (2001); Phys. Rev. Lett. **89**, 201802 (2002); Phys. Rev. Lett. **94**, 161803 (2005).
  - [7] Heavy Flavor Averaging Group, J. Alexander *et al.*, hep-ex/0412073.
  - [8] Y. Grossman and M. P. Worah, Phys. Lett. B **395**, 241 (1997); D. London and A. Soni, Phys. Lett. B **407**, 61 (1997).

- [9] A. G. Akeroyd *et al.*, hep-ex/0406071 and references therein.
- [10] Belle Collaboration, K. Abe *et al.*, Phys. Rev. D **72**, 012004 (2005).
- [11] BaBar Collaboration, B. Aubert *et al.*, Phys. Rev. Lett. **94**, 041802 (2005); Phys. Rev. Lett. **94**, 191802 (2005); Phys. Rev. D **71**, 091102 (2005); Phys. Rev. D **71**, 111102 (2005).
- [12] T. Gershon and M. Hazumi, Phys. Lett. B **596**, 163 (2004).
- [13] Belle Collaboration, A. Garmash *et al.*, Phys. Rev. D **69**, 012001 (2004).
- [14] S. Kurokawa and E. Kikutani, Nucl. Instr. and Meth. A **499**, 1 (2003).
- [15] Belle Collaboration, A. Abashian *et al.*, Nucl. Instr. and Meth. A **479**, 117 (2002).
- [16] Y. Ushiroda (Belle SVD2 Group), Nucl. Instr. and Meth. A **511**, 6 (2003).
- [17] Belle Collaboration, B.C.K. Casey *et al.*, Phys. Rev. D **66**, 092002 (2002).
- [18] ARGUS Collaboration, H. Albrecht *et al.*, Phys. Lett. B **241**, 278 (1990).
- [19] H. Kakuno *et al.*, Nucl. Instr. and Meth. A **533**, 516 (2004).
- [20] H. Tajima *et al.*, Nucl. Instr. and Meth. A **533**, 370 (2004).
- [21] S. Eidelman *et al.*, Phys. Lett. B **592**, 1 (2004).
- [22] O. Long, M. Baak, R. N. Cahn and D. Kirkby, Phys. Rev. D **68**, 034010 (2003).
- [23] G. J. Feldman and R. D. Cousins, Phys. Rev. D **57**, 3873 (1998).
- [24] BaBar Collaboration, B. Aubert *et al.*, Phys. Rev. Lett. **95**, 011801 (2005).